Liquid Crystals

Publication details, including instructions for authors and subscription information:
http://www.informaworld.com/smpp/title~content=t713926090

Inverse Langmuir-Schaefer films of bent-core molecules

Ji Wang[a]; Liou Qiu[b]; Antal Jákli[b]; Wolfgang Weissflog[c]; Elizabeth K. Mann[a]
[a] Department of Physics, Kent State University, Kent, OH, USA [b] Liquid Crystal Institute, Kent State University, Kent, OH, USA [c] Institut für Physikalische Chemie, Universität Halle-Wittenberg, Halle, Germany

To cite this Article Wang, Ji , Qiu, Liou , Jákli, Antal , Weissflog, Wolfgang and Mann, Elizabeth K.(2010) 'Inverse Langmuir-Schaefer films of bent-core molecules', Liquid Crystals, 37: 10, 1229 — 1236

To link to this Article: DOI: 10.1080/02678292.2010.494739

URL: http://dx.doi.org/10.1080/02678292.2010.494739

Liquid Crystals,
Vol. 37, No. 10, October 2010, 1229–1236

Inverse Langmuir–Schaefer films of bent-core molecules

Ji Wang[a], Liou Qiu[b], Antal Jákli[b], Wolfgang Weissflog[c] and Elizabeth K. Mann[a]*

[a]*Department of Physics, Kent State University, Kent, OH, USA;* [b]*Liquid Crystal Institute, Kent State University, Kent, OH, USA;* [c]*Institut für Physikalische Chemie, Universität Halle-Wittenberg, Halle, Germany*

(*Received 10 February 2010; final version received 17 May 2010*)

Mesostructures in inversed Langmuir–Schaefer films of each of two contrasting bent-core molecules are explored via atomic force microscopy. One of the molecules forms Langmuir films that are optically isotropic and the other those that are optically anisotropic. Both show suboptical mesostructures in the 100 nm range, in spite of appearing optically uniform. The anisotropic films are effective in aligning nematic bent-core samples, but not rod-like liquid crystals such as 5CB.

Keywords: bent-core molecules; thin films; Langmuir–Schaefer films; alignment layers

1. Introduction

Liquid crystals of bent-core molecules [1] form a large number of smectic and columnar phases that are denoted by B1 . . . B7 according to the chronological order of their discovery [2–4]. Their tilted smectic [5] and columnar [6] phases are chiral without chiral stereo-centres being incorporated into their molecules, and possess ferroelectric and antiferroelectric structures which can be switched in times well below a millisecond. These properties make them very attractive for practical applications [7] such as electromechanical [8] or electro-optical display devices or in various kinds of organic devices [9]. Due to the molecular shape of the bent core, and because they do not typically form nematic phases above the smectic phases, these molecules cannot be aligned with conventional techniques such as rubbed polyimide [10, 11] or nylon. Although in some cases – for example when switching between transparent and scattering states [12] – alignment is irrelevant, its lack often prohibits practical applications. This difficulty highlights the fundamental interest of studying molecular interactions of bent-core molecules with surfaces. Thin films for such studies, and for potential alignment layers with molecular structures similar to the bent-core molecules to be aligned, can be prepared by vacuum deposition, self-assembly or Langmuir–Blodgett (LB) deposition techniques.

Thin films of the simplest, three-ring, bent-core molecules were vacuum-deposited on mica substrates by Tang *et al.* [9, 13]. Their morphologies, structures and phase behaviour, investigated by atomic force microscopy (AFM) and transmission electron microscopy (TEM), demonstrated the formation of films with (anti-)ferroelectricity. A series of five-ring, bent-core molecules (same cores, different end-chains) were self-assembled on highly-oriented Pyrolytic graphite (HOPG) and studied using scanning tunnelling microscopy (STM) [14]; well-organised stripes were observed. Bent-core molecules have also recently been covalently attached to silicon surfaces [15]. These studies demonstrated that not only interactions between the molecules, but also molecule–substrate interactions play important roles in forming uniform films. In Langmuir films one can freely and directly vary the average molecular area and other film conditions allowing the creation of a wide range of optically anisotropic phases where the orientation can be controlled by the compression and deposition conditions [16].

To the best of our knowledge, five sets of articles have considered Langmuir films of bent-core molecules. The first dealt with a single bent-core molecule with long hydrophobic side chains [17]. The second, published by Blinov and co-workers [18–20], investigated the dielectric, ferro- and antiferroelectric properties of LB films of similar bent-core molecules. A third set of articles described two different cores with very short hydrophobic side chains [21, 22]. The fourth, very recent article, considered the structure of films of fluorinated molecules [23]. Earlier work in our laboratory [24] concerned Langmuir films of five bent-core molecules, varying both the core and the end-chains but maintaining molecular symmetry with identical end-chains on either end of the core. The characterisation included systematic surface pressure isotherms, Brewster angle microscopy (BAM) [25, 26] and surface potential measurements; the combination of techniques demonstrated stable Langmuir films of a variety of different bent-core molecules. It was found

---

*Corresponding author. Email: emann@kent.edu

ISSN 0267-8292 print/ISSN 1366-5855 online

DOI: 10.1080/02678292.2010.494739
http://www.informaworld.com

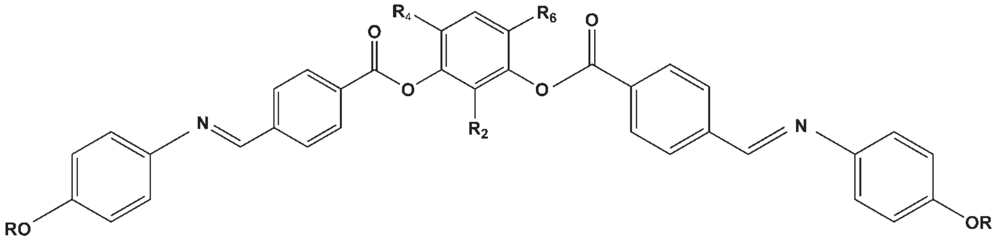

Figure 1. Molecular formulae for Bc-2Cl and Bc-NO_2; see Table 1 for the identities of R_n. Space filling molecular models suggest dimensions 4.6 nm × 1.6 nm.

Table 1. Molecule formulae for Bc-2Cl and Bc-NO_2.

Identifier	R_2	R_4	R_6	R	Phase sequence in bulk	Reference
Bc-2Cl	H	Cl	Cl	C_9H_{19}	Cr 106°C (SmC 88°C) N 143°C I	[35]
Bc-NO_2	NO_2	H	H	C_8H_{17}	Cr 116 B_7 177 I	[2–4]

that molecules with siloxane end-chains lie quite flat on the surface, with both core and end-chains in direct contact with the air/water interface, whereas molecules with hydrophobic chains, with their weaker attraction to the water surface, form complex multilayer structures at even very low pressures. A very similar bent-core molecule, but with two chlorine atoms attached on the outside of the centre phenyl ring (positions 4 and 6, as shown in Figure 1), were found [16] to pack anisotropically, in contrast to materials that had hydrogen atoms on the outside and any one of several groups substituted in the inner angle of this phenyl ring (position 2 as shown in Figure 1), and which all appeared optically isotropic [24]. In the optically anisotropic films, the anisotropy appeared to be independent of the film thickness (or number of layers). X-ray reflectivity [27] suggested that even the films that appeared optically smooth were, at a molecular level, quite rough. Many questions remained: while the mean molecular area at which the pressure increased measurably demonstrated that the films were clearly more than one molecule thick, the film structure could only be speculated upon. Are the films regularly layered and, if so, what is the molecular conformation within each layer? What is the nature of the film roughness at scales below the optical scale?

In this paper we explore by AFM the mesostructures of Langmuir films of bent-core molecules transferred to a solid interface by LB and related methods. We further see clear evidence of discrete layers in annealed films, and measure the height difference between layers for evidence of molecular orientation within the layers. To explore the use of these molecules as alignment layers, we also investigate the alignment they impose on rod-shaped and bent-core liquid crystals.

2. Methods and materials

The chemical structures of the bent-core molecules studied, called Bc-2Cl and Bc-NO_2 as in [16, 24], are shown in Figure 1. The material is deposited with a chloroform (Aldrich, A.C.S, high-performance liquid chromatography grade) spreading solution onto a pure water surface. Water was purified with a Purelab Plus UV system (US Filter, resistivity 18.2 MΩ·cm), and held in a homemade Teflon minitrough, which performed well in tests against leakage around the hydrophilic barriers from KSV Instruments. The minitrough was cleaned with KOH solution (KOH 25 g, water 24 g, C_2H_6O 136 g), and rinsed copiously with pure water. The Langmuir films were formed at 17 ± 1°C with ~50% humidity. The surface pressure measurements were performed via the Wilhelmy method [28].

Langmuir films of bent-core molecules were transferred to a solid substrate placed under the surface before deposition and then raised a few degrees from the horizontal with respect to the water surface, to form what are called inverse Langmuir–Schaefer (ILS) films. The more commonly used LB methods (vertical transfer) were not successful for the hydrocarbon end-chain molecules studied here because the films are brittle. Films were transferred at several different portions of the compression isotherm, as indicated below, in order to test for any mesostructure and anisotropy in that mesostructure. In order to test the overall thickness of the films, films were also transferred after a slight decompression until the surface pressure decreased to zero, and the films broke into optically uniform fragments with a very dilute gaseous monolayer between them. The ILS films on mica were observed using the NanoScope III Atomic Force Microscope. ILS films on glass were glued face to face using 5 µm spacers to make thin sandwich cells. A bulk sample of a well-studied bent-core liquid crystal 4-chloro-1,3-phenylene bis [4-(10-decenyloxy) benzoyloxy] benzoate (ClPbis10BB [29]) with a nematic phase between 74°C and 54°C on cooling was then introduced at 90°C from the edge into the cell by capillarity. Polarising microscopy (BX60 from Olympus) was used to check the alignment within the cell.

3. Experimental results

3.1 AFM microscopy of ILS films

In interpreting images of Langmuir films transferred to a solid substrate, it is important to remember that the transfer may change the properties of the film. Material may migrate on the substrate, to change film conditions [30–33]. Alignment by flow during the transfer process may be an advantage for fluid films [34]. In stiff multilayers of the kind observed here, the major changes should be cracking of the films, leaving the internal structure unchanged. The AFM thus allowed us to explore structures on the 0.02–10 µm scale that are probably representative of both the transferred films and the original film on the water surface.

3.1.1 Isotropic films

Most of this work concerns a bent-core molecule, Bc-2Cl, that forms optically anisotropic films promising for alignment purposes. For comparison, first consider films made of Bc-NO_2, a similar molecule that forms isotropic Langmuir films on the water surface. Note the granular appearance of the AFM image of Bc-NO_2 (Figure 2) films transferred to a mica substrate. This film was transferred at the first decompression just after the surface pressure π decreases to zero, where the Langmuir film is optically smoothest. There is little obvious structural anisotropy in the AFM images, but the structure, while irregular, shows a definite characteristic size and organisation over the whole region. The fast Fourier transform (FFT, inset of Figure 2) shows a distorted hexagonal lattice. The two primitive vectors of the hexagonal structure are 100 nm and 60 nm in real space, corresponding to a rectangular structure with a ratio of width over height of ~1.65 ± 0.1. This ratio is close to the X-ray results for a bulk smectic phase of a very similar bent-core molecule, with a CH_3 replacing the NO_2 group in the R_2 position in Figure 1 [35], with

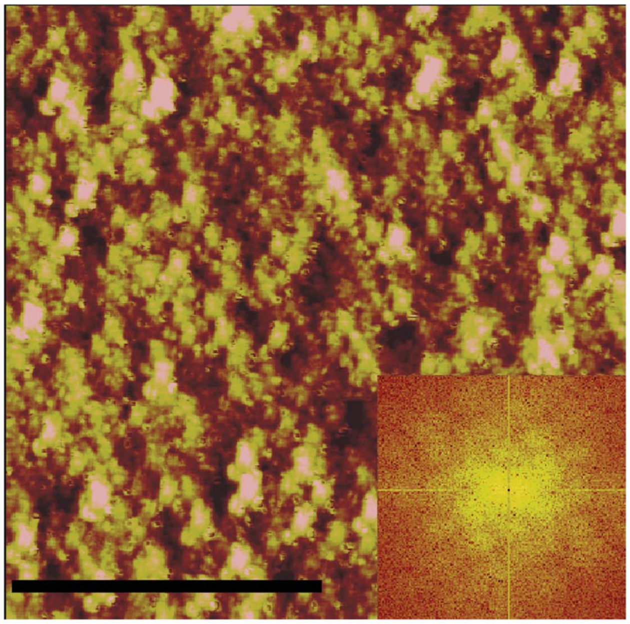

Figure 2. AFM image of Bc-NO_2 ILS film transferred after decompression just until the surface pressure π decreases to near zero. The bar corresponds to 1 µm and the colour scale dark to light corresponds to a 5 nm increase in height. The inset is the FFT of the image (colour version online).

characteristic scales of ~1 nm. The structure observed by AFM thus appears to reflect the underlying molecular-scale organisation, but at a scale 25 times larger.

3.1.2 Anisotropic films

Langmuir films of Bc-2Cl were transferred to mica at different pressures as shown in the isotherm in Figure 3. Representative films of Bc-2Cl were taken: (1) at the co-area, defined as the area per molecule where the pressure starts to increase significantly; (2) where a shoulder appears in the surface pressure, ~17 mN m^{-1}; (3) close to the end of the compression, above 30 mN m^{-1}, where thick defect lines appear. Langmuir films were also transferred onto clean glass substrates, and tested as alignment layers for another type of nematic bent-core molecules; the results from polarising microscopy, under crossed polarisers, are also given in Figure 3. Note that in all cases small domains of different thickness appear as in the BC-NO$_2$ case, but here these domains are visibly anisotropic and aligned.

The three AFM images shown in Figure 3 are typical of three different regions, with different film morphologies. Each will be discussed individually as follows.

Region I: From just after deposition (Figure 4(a)) to the co-area region (in Figure 3). At deposition, the Bc-2Cl molecules pack spontaneously on the water surface without any external forces, except the local ones exerted during the spreading and evaporation of the spreading solvent. The surface of the film is divided into small (~50–200 nm width) grains aligned parallel to each other (Figure 4(a)). The FFT (Figure 4(a), inset) of this image demonstrates more quantitatively the alignment, with an elongated spot with aspect ratio 4:1, as determined by the half-width at half-maximum intensity. Note that this alignment might happen during the initial Langmuir deposition, when the droplet of the solution spreads and then contracts in a locally regular way. It could also be induced during the ILS deposition process, by flow of the underlying fluid [34].

Region II: Between about 5 mN m^{-1} and 17 mN m^{-1}, at the isotherm shoulder. The surface pressure starts increasing at $\sigma = 0.28$ nm^2/molecule (co-area). Small domains are observed by AFM in films transferred at the lowest pressures; at larger pressures these domains are wider, until, near the shoulder, a flat plateau with deep crevices is seen (Figure 3 for a surface pressure $\pi \sim 15$ mN m^{-1}). The crevices join each other at an angle, many of them between 140° and 150°, although smaller angles also appear. These angles may reflect the underlying molecular order of the film, and should be compared to both the observed bending angle of Bc-2Cl in bulk [36], 165°, and the simple hexagonal lattice (60, 120°).

Region III: Films deposited after the shoulder to the end of the compression. As the pressure increases more rapidly, after the shoulder, many small grain-shaped domains again appear (Figure 4(b)) in the deposited films, in a herringbone-like structure. The FFT image (inset in Figure 4(b)) shows clear anisotropy, with a preferred direction (34° with respect to the compressing barriers) and a repeat distance of ~30 nm. When deposited at $\pi \sim 35$ mN m^{-1}, folds in the film appear, as shown in Figure 3. These correspond to optical defect lines approximately parallel to the barriers. To view film details, a smaller area 2 μm × 2 μm is scanned as shown in Figure 4(c). Large (~120 nm width) grain-shaped domains are seen; the FFT demonstrates that some alignment of the domains persists. The anisotropy

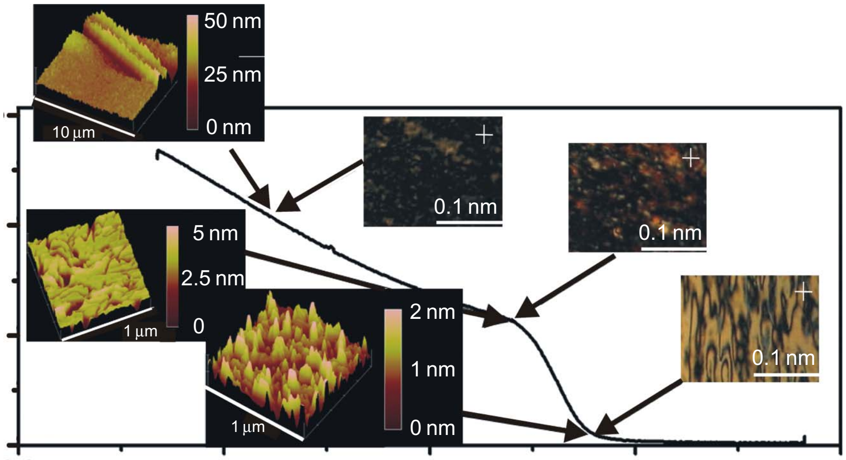

Figure 3. The effect of compression on Bc-2Cl film structures as determined by AFM on films transferred to mica (images to left) and alignment of a nematic liquid crystal 4-chloro- 1,3-phenylene bis [4-(10-decenyloxy) benzoyloxy] benzoate (ClPbis10BB) [37] by films transferred to glass (images to right of curve). The crosses indicate the direction of the polariser and the analyser. Note that the alignment is more effective the more the film has been compressed, even as the films develop defects (colour version online).

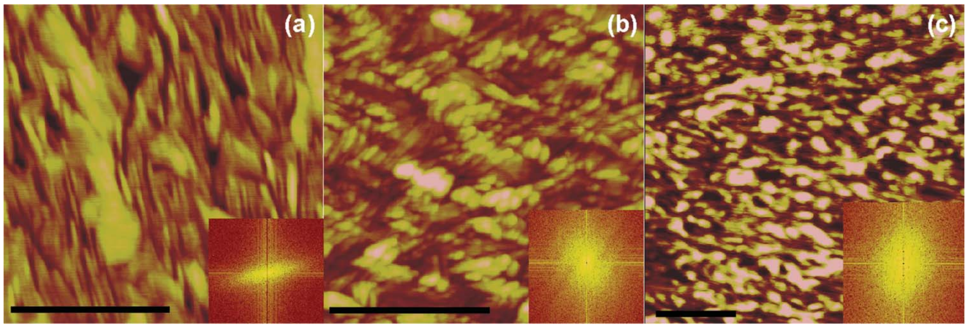

Figure 4. (a) Bc-2Cl ILS film just after deposition; (b) Bc-2Cl ILS film transferred with $\pi \sim 21$ mN m^{-1}; (c) Bc-2Cl ILS film transferred with $\pi \sim 35$ mN m^{-1}. The bars correspond to 0.5 μm and the colour range corresponds to 8 nm. Insets are the FFTs of the image; these are anisotropic with length:width ratios (a) 4:1,(b) 1.3:1 and (c) 1.6:1.

direction is within ±15° with respect to the defect lines, and therefore approximately parallel to the barriers. The alignment may thus be caused by the compression.

3.2 *Film thickness characterisation*

Judging by the co-area, Langmuir films of Bc-2Cl were several (two to three) molecules thick before a surface pressure registered [16]. While transferred films appeared very granular at the meso-scale, the original films on water (Figure 5(a)) were sufficiently uniform on the scale greater than 10 μm to provide consistent, reasonable values for optical thickness and anisotropy [16]. However, the actual thickness of these films could not be directly determined from the optical measurements.

Film thicknesses were directly determined by AFM from ILS films transferred from Langmuir films that were first fully compressed and then slightly decompressed, so that the film broke into several parts. The resulting fragments were nearly uniform and in coexistence with a gaseous film. The most extensive optical results [16], showing optically uniform films with fixed anisotropy, were taken under these conditions. Such fragments, at zero pressure, are also unlikely to be changed by the transfer process. A film with several small pieces and blank space between them allowed us to measure the height difference between the mica and the film (Figure 5(b)). This height is about 15 nm, consistent with the earlier film thickness analysis from the mean molecular area at which the pressure dropped, assuming bulk densities. However, the film is much less uniform than the optical pictures (Figure 5(a)), and the consistency of the observed optical thickness, suggest.

When scanning the film with greater resolution, as shown in Figure 5(c), islands about 15 nm in thickness and $\sim$50–100 nm in size are clearly seen. Note that this film was deposited at a similar average molecular area as the film in Figure 2, so that the average film thickness of this film is similar. However, the height difference between the brightest and darkest part is more than that shown in Figure 2, which indicates that the Bc-2Cl film is rougher than the Bc-NO$_2$ film. In both cases, these islands must pack surprisingly uniformly to yield the apparent uniformity in optical thickness (illustrated in Figure 5(a)). The islands must include many single molecules, with dimensions $\sim$4.6 nm ×

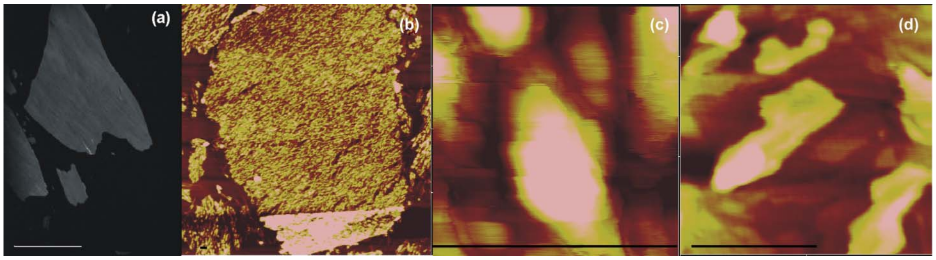

Figure 5. (a) The Langmuir film of Bc-2Cl observed under BAM with $\sigma \sim 0.19$ nm^2/molecule at the first decompression; the scale bar is 1 mm. (b) An AFM image of Bc-2Cl ILS film transferred at the same molecular area; the picture has dimensions 10 μm × 10 μm. The scale bars on all AFM images represent 0.25 μm. (c) A close-up of the same film; the colour scale is 0–12 nm. (d) An AFM image of a film transferred under the same conditions after annealing for 15 min. The colour scale is 0–8 nm.

1.6 nm. How these molecules pack together in such a configuration and what constrains the island size remains a question.

3.3 Single-layer thickness analysis after annealing

The thickness of a single layer, if such a layer exists, would be useful information for determining the molecular orientation and packing structure. Annealing is one way to help the molecule find the lowest energy level. The ILS film as shown in Figure 5 was heated at 88°C for either 15 min, shown in Figure 5(d), or 1 h. It is obvious that after annealing the rough film shown in Figure 5(c) becomes much smoother and plateaus of different thickness are clearly observed. However, this is not an equilibrium structure, since the longer annealing leads to a greater number of plateau regions that are smaller across, with less well-defined angles.

Preliminary film thickness analysis has been done on both films. The film thicknesses seem to be multiple numbers of 0.6 nm. Note 0.6 nm is approximately the dimension of a phenyl ring or the nominal thickness of a molecule. This observation suggests that the films consist of multiple layers of molecules lying relatively flat on the surface.

3.4 Using ILS films as alignment layers for liquid crystal cells

Three liquid crystal cells were made with Bc-2Cl Langmuir film transferred with different surface pressure as shown in Figure 3. These cells were observed under a cross-polarised microscope (BX60 from Olympus) after filling in with a nematic bent-core liquid crystal 4-chloro-1,3-phenylene bis [4-(10-decenyloxy) benzoyloxy] benzoate (ClPbis10BB) [37]; the textures are shown in Figure 3 (right-hand side of curve). ClPbis10BB has one chlorine atom in the 4 position of the central benzene ring, and the benzene rings in the molecular arms are separated by ester groups. It exhibits a monotropic nematic phase on cooling between 73°C and 53°C. This material has been the subject of several studies so that its main physical parameters have been determined [38, 39]. It exhibits giant flexoelectricity with a coefficient over three orders of magnitude larger than that in calamitic liquid crystals [40].

To best judge the alignment of the bulk nematic liquid crystal by the ILS film, the cells were rotated to find the darkest field. A completely dark image implies that all of the liquid crystal is aligned with either the analyser or polariser, while any variation in colour means that different parts of the cell are oriented in different directions. All cases show parallel alignment, while a bare glass surface leaves randomly oriented regions instead. The textures with the best alignment are similar to those observed with rubbed polyimide as the alignment layer. From these images we also see that the alignment is more effective the more the film has been compressed, even though in this range the AFM studies showed that the films developed defects. Finally, the alignment of the bent-core nematic material was found to be stable over several months, suggesting that any changes in the alignment layer with time in contact with the nematic have a minor effect.

4. Discussion

As shown in the AFM images of Bc-2Cl, we found that, instead of packing together uniformly in a wide area, the molecules form elongated clusters with dimensions ~50 nm × 150 nm, which packed together with small gaps in between. Due to the small dimensions of these clusters, they are not visible under the red laser (wavelength ~668 nm) used for the BAM microscopy on the original Langmuir films. This kind of mesostructure has also been found for a different bent-core molecule [41], where the dimension of the mesostructure was reported to be ~30 nm, which is slightly smaller than the value we found in Bc-2Cl.

We have also observed an anisotropic arrangement of small surface grains in the ILS film of Bc-2Cl. No similar structural anisotropy was found in the ILS film of Bc-NO_2. Note that the structural anisotropy is different for the different cases shown above (Figure 3). We note also that, comparing Figures 4(a) and 4(c), the structural anisotropy of the grains and grain arrangement appears to *decrease* as the film is compressed. This difference does not seem to be reflected in the macroscopic optical anisotropy. It is thus likely that the two effects, structural anisotropy and the anisotropy in the refractive index, are not related by cause and effect, but rather both due to a regular anisotropic molecular packing pattern. Note that little structural anisotropy is seen for other hydrocarbon end-chain bent-core molecules, consistent with its lack of optical anisotropy; the combination suggests an underlying isotropic molecular packing pattern [24].

In many regimes, some scale selection for the mesodomains was observed, especially for Bc-NO_2, where the structures were surprisingly well-ordered. It is unclear whether this scale is a natural one or kinetically determined. The possibility that the transfer process produces these domains must be considered, but an important transfer effect seems unlikely for these immobile multilayers. A more likely possibility is that these mesostructures reduce either the polarity or the elastic strain in the partially ordered film. Indeed, modulated structures have been observed by X-ray diffraction in a number of bulk bent-core liquid crystalline phases [42, 43].

In all cases, we observe films with thicknesses characteristic of multilayers. Annealing the Bc-2Cl film yields a 0.6 nm film periodicity, characteristic of a benzene ring. This suggests that the molecules are lying quite flat on the water, which is consistent with recent atomistic molecular dynamics simulations of one [44] or two [45] such molecules at the water surface.

Importantly, the actual alignment of the bent-core nematic phase by the Bc-2Cl ILS film deposited at 0.13 nm^2/molecule specific area is almost completely uniform. This is remarkable, especially since the classical liquid crystal octyl cyano biphenyl (8CB), which can readily be aligned in a classic rubbed cell or by a variety of other methods, was not aligned by the Bc-2Cl ILS film. Two main pictures exist for liquid crystal alignment by a surface. The Berreman model suggests that the substrate surface shape, and in particular microgrooves, favours a particular alignment through elastic energy [46]. Experiments suggest that a more subtle property of the surface roughness, its anisotropy, is the critical parameter [47]. The other major model for alignment [48], supported by recent simulations [49], suggests that direct molecular interactions are the more important player. For example, the aliphatic chains of a liquid crystal may penetrate a similar film on the surface, and adapt the orientation of those chains [50].

Our result is consistent with alignment by direct interactions with the surface film. Such interactions are more likely to provide a unique alignment direction when the molecules in the liquid crystal and the surface film are similar in shape. With the bent-core surface molecules lying quite flat on the surface, the two hydrocarbon chains and the two core wings would be at very different in-plane angles, and thus would not provide a consistent set of interactions to align a more linear molecule in a single direction, yet they could provide an appropriate set of interactions to align molecules of similar shape. By the same reasoning, small rod-shaped molecules could form tilted bilayers, aligning with each half of the bent-core molecules, which could explain the inability of these layers to align 5CB.

Acknowledgements

We thank Katalin Fodor-Csorba for providing ClBbis 10BB for us. We would also like to thank a very helpful referee for significant suggestions. The work was sponsored by NSF-DMR 0907055.

References

[1] Niori, T; Sekine, T.; Watanabe, J.; Furukawa, T.; Takezoe, H. *J. Mater. Chem.* **1996**, *6*, 1231–1233.
[2] Pelzl, G.; Diele, S.; Weissflog, W. *Adv. Mater.* **1999**, *11*, 707–724.
[3] Takezoe, H.; Takanishi, Y. *Jpn. J. Appl. Phys.* **2006**, *45*, 597–625.
[4] Reddy, R.A.; Tschierske, C. *J. Mater. Chem.* **2006**, *16*, 907–961.
[5] Link, D.R.; Natale, G.; Shao, R.; Maclennan, J.E.; Clark, N.A.; Körblova, E.; Walba, D.M. *Science* **1997**, *278*, 1924–1927.
[6] Gorecka, E.; Vaupotic, N.; Pociecha, D.; Cepic, M.; Mieczkowski, D. *Chem. Phys. Chem.* **2005**, *6*, 1087–1093.
[7] Etxebarria, J.; Ros, M.B. *J. Mater. Chem.* **2008**, *18*, 2919–2926.
[8] Jákli, A.; Krüerke, D.; Nair, G.G. *Phys. Rev. E: Stat., Nonlinear, Soft Matter Phys.* **2003**, *67*, 051702.
[9] Tang, T.H.; Wang, Y.; Wang, G.; Wang, H.B.; Wang, L.X.; Yan, D.H. *J. Phys. Chem. B* **2004**, *108*, 12921–12926.
[10] Mauguin, C. *Bull. Soc. Fr. Mineral.* **1911**, *34*, 71–111.
[11] Cognard, J. *Mol. Cryst. Liq. Cryst. Suppl. Ser.* **1982**, *1*, 1–77.
[12] Jákli, A.; Krüerke, D.; Sawade, H.; Chien, L.C.; Heppke, G. *Liq. Cryst.* **2002**, *29*, 377–381.
[13] Tang, Y.H.; Wang, Y.; Wang, X.D.; Xun, X.D.; Mei, C.Y.; Wang, L.X.; Yan, D.H. *Phys. Chem. B* **2005**, *109*, 8813–8819.
[14] Gong, J.R.; Wan, L.J. *J. Phys. Chem. B* **2005**, *109*, 18733–18740.
[15] Scheres, L.; Achten, R.; Giesbers, M.; de Smet, L.C.P.M.; Arafat, A.; Sudhölter, E.J.R.; Marcelis, A.T.M.; Zuilhof, H. *Langmuir* **2009**, *25*, 1529–1533.
[16] Wang, J.; Zou, L.; Jakli, A.; Weissflog, W.; Mann, E.K. *Langmuir* **2006**, *22*, 3198–3206.
[17] Kinoshita, Y.; Park, B.; Takezoe, H.; Niori, T.; Watanabe, J. *Langmuir* **1998**, *14*, 6256–6260.
[18] Blinov, L.M.; Geivandov, A.R.; Lazarev, V.V.; Palto, S.P.; Yuding, S.G.; Pelzl, G.; Weissflog, W. *Appl. Phys. Lett.* **2005**, *87*, 241913.
[19] Blinov, L.M.; Palto, S.P.; Lazarev, V.B.; Geivandov, A.R.; Yuding, S.G *Crystallograph.* **2006**, *51*, 843–849.
[20] Geivandov, A.R.; Palto, S.P.; Yudin, S.G.; Blinov, L.M.; Pelzl, G.; Weissflog, W. *Ferroelectrics* **2006**, *344*, 247–254.
[21] Ashwell, G.J.; Amiri, M.A. *J. Mater. Chem.* **2002**, *10*, 2181–2183.
[22] Baldwin, J.W.; Amaresh, R.R.; Peterson, I.R.; Shumate, W.J.; Cava, M.P.; Amiri, M.A.; Hamilton, R.; Ashwell, G.J.; Metzger, R.M. *J. Phys. Chem. B* **2002**, *106*, 12158–12164.
[23] Garcia-Vazquez, P.; Morales-Saavedra,O.G.; Pelzl, G.; Guadalupe Bañuelos, J.; Carreón-Castro, M.P. *Thin Solid Films* **2009**, *517*, 1770–1777.
[24] Zou, L.; Wang, J.; Beleva, V.; Kooijman, E.E.; Primak, S.V.; Risse, J.; Weissflog, W.; Jákli, A.; Mann, E.K. *Langmuir* **2004**, *20*, 2772–2780.
[25] Hénon, S.; Meunier, J. *Rev. Sci. Instrum.* **1991**, *62*, 936–939.
[26] Hönig, D.; Möbius, D. *J. Phys. Chem.* **1991**, *95*, 4590–4592.
[27] Wang, J.; Zou, L.; Basnet, P.; Vaknin, D.; Mann, E.K. Unpublished Work.
[28] Adamson, A.W.; Gast, A.P. *Physical Chemistry of Surfaces*, 6th ed.; Wiley: New York, 1997.
[29] Fodor-Csorba, K.; Jákli, A.; Galli, G. *Macromol. Symp.* **2004**, *218*, 81–88.

[30] Riegler, H.; Spratte, K. *Thin Solid films* **1992**, *210*, 9–12.

[31] Sikes, H.D.; Schwartz, D.K. *Langmuir* **1997**, *13*, 4704–4709.

[32] Schwartz, D.K. *Surface Sci. Rep*. **1997**, *27*, 245–334.

[33] Vickery, S.A.; Dunn, R.C. *Langmuir* **2001**, *17*, 8204–8209.

[34] Friedenberg, M.C.; Fuller, G.G.; Frank, C.W.; Robertson, C.R. *Macromolecules* **1996**, *29*, 705–712.

[35] Diele, S.; Grande, S.; Kruth, H.; Lischka, C.; Pelzl, G.; Weissflog, W.; Wirth, I. *Ferroelectrics* **1998**, *212*, 169–177.

[36] Weissflog, W.; Lischka, C.; Diele, S.; Pelzl, G.; Wirth, I.; Grande, S.; Kresse, H.; Schmalfuss, H.; Hartung, H.; Stettler, A. *Mol. Cryst. Liq. Cryst*. **1999**, *333*, 203–223.

[37] Fodor-Csorba, K.; Jákli, A.; Galli, G. *Macromol. Symp*. **2004**, *218*, 81–88.

[38] Wiant, D.B.; Gleeson, J.T.; Eber, N.; Fodor-Csorba, K.; Jákli, A.; Toth-Katona, T. *Phys. Rev. E: Stat., Nonlinear, Soft Matter Phys*. **2005**, *72*, 041712.

[39] Wiant, D.; Stojadinovic, S.; Neupane, K.; Sharma, S.; Fodor-Csorba, K.; Jákli, A.; Gleeson, J.T.; Sprunt, S. *Phys. Rev. E: Stat., Nonlinear, Soft Matter Phys.* **2006**, *73*, 030703.

[40] Harden, J.; Mbanga, B.; Éber, N.; Fodor-Csorba, K.; Sprunt, S.; Gleeson, J.T.; Jákli, A. *Phys. Rev. Lett*. **2006**, *97*, *157802*.

[41] Liao, G.; Stojadinovic, S.; Pelzl, G.; Weissflog, W.; Sprunt, S.; Jákli, A. *Phys. Rev. E: Stat., Nonlinear, Soft Matter Phys*. **2005**, *72*, 021710.

[42] Reddy, R.A.; Tschierske, C. *J. Mater. Chem*. **2006**, *16*, 907–961.

[43] Szydlowska, J.; Mieczkowski, J.; Matraszek, J.; Bruce, D.W.; Gorecka, E.; Pociecha, D.; Guillon, D. *Phys. Rev. E: Stat., Nonlinear, Soft Matter Phys*. **2003**, *67*, 031702.

[44] Duff, N.; Wang, J.; Mann, E.K.; Lacks, D.J. *Langmuir* **2006**, *22*, 9082–9085.

[45] Duff, N.; Mann, E.K.; Lacks, D.J. *Langmuir* **2008**, *24*, 4456–4460.

[46] Berreman, D.W. *Phys. Rev. Lett*. **1972**, *28*, 1683–1686.

[47] Kumar, S.; Kim, J.H.; Shi, Y. *Phys. Rev. Lett*. **2005**, *94*, 077803.

[48] Lee, E.S.; Saito, Y.; Uchida, T. *Jpn. J. Appl. Phys. 2-Lett*. **1993**, *32*, L1822–L1825.

[49] Hamaneh, E.B.; Taylor, P.L. *Phys. Rev. E: Stat., Nonlinear, Soft Matter Phys*. **2008**, *77*, 021707.

[50] Jérôme, B. In *Physical Properties of Liquid Crystals*: Demus, D., Goodby, J., Gray, G.W., Spiess, H.-W., Vill, V., Eds.; Wiley: New York, 1990; Chapter 10, p 434.